

# Preparation and Modification of MIL-101(Cr) Metal Organic Framework and Its Application in Lithium-Sulfur Batteries

Guangjie Gao<sup>2</sup>, Wangjun Feng<sup>1,2,\*</sup>, Wenxiao Su<sup>2,3,\*</sup>, Shejun Wang<sup>3</sup>, Linjing Chen<sup>2</sup>, Miaomiao Li<sup>2</sup>, Changkun Song<sup>2</sup>

<sup>1</sup> State Key Laboratory of Advanced Processing and Recycling Nonferrous Metals, Lanzhou University of Technology, Lanzhou 730050, China;

<sup>2</sup> School of Science, Lanzhou University of Technology, Lanzhou 730050, China

<sup>3</sup> Department of Basic Course, Lanzhou Institute of Technology, Lanzhou 730050, China)

\*E-mail: [wjfeng@lut.cn](mailto:wjfeng@lut.cn) (W.J. Feng), [suwx@lzit.edu.cn](mailto:suwx@lzit.edu.cn) (S.W.Xiao).

Received: 7 September 2019 / Accepted: 18 November 2019 / Published: 31 December 2019

---

Lithium sulfur batteries have high theoretical specific capacity and good application prospects. In this paper, large surface area mesoporous chromium MIL-101 (Cr) metal organic framework has been prepared by hydrothermal method and composite with carbon nanotubes (CNTs) as the host of sulfur. The composite electrode material of MIL-101@CNT/S shows the excellent electrochemical performance. Especially the MIL-101@5%CNT/S composite electrode material, when the current density at 0.1C, it has a high initial discharge capacity of 1236.7 mA h g<sup>-1</sup>, and its specific capacity retention rate reaches 53.4% after 200 cycles. What's more, thanks to the addition of CNTs, the results have better high multiplier performance than MIL-101 (Cr)/S, and the capacity contributed by the second platform has been improved.

---

**Keywords:** MIL-101(Cr); Lithium-sulfur battery; CNTs; Shuttle effect.

## 1. INTRODUCTION

Traditional transition metal oxide lithium ion batteries can't meet the high energy density requirements for electrical appliances. Therefore, it is urgent to develop batteries with high energy density and safety[1]. Lithium sulfur batteries have attracted extensive attention due to their high theoretical specific capacity (1675mA·h/g) and high theoretical energy density (2600W·h/kg)[2]. Besides, sulfur is not only a suitable cathode material, but also has the advantages of natural abundance and environmentally friendly[2–4]. However, there are still many limitations in the practical application of lithium-sulfur batteries. (1) The generation of high solubility polysulfide causes serious shuttle effect between cathode and metal lithium anode, resulting in low coulomb efficiency

and capacity attenuation[2,5]. (2) As sulfur and reduction products are insulators at room temperature, the utilization rate of sulfur is reduced and the actual capacity is low[2,6]. (3) The volume expansion of sulfur cathode is obvious during charging and discharging, which leads to insufficient cycle life. (4) The final products of sulfur electrochemical reduction ( $\text{Li}_2\text{S}$  and  $\text{Li}_2\text{S}_2$ ) are insoluble insulating substances, which tend to block the electron and ion transport channels of sulfur anode.

The main problems to be solved urgently for lithium sulfur battery are the poor conductivity of anode material and the dissolution and diffusion of polysulfide. In order to overcome these problems, researchers take many useful measures to design and modification the host of sulfur for Li-S batteries, such as porous cathode[7–9], porous carbon[10–13], conductive polymer [14,15], metal organic framework (MOFs)[16–18] and other types of porous materials.

Carbon materials in composite electrode materials have two main functions: one is to provide electrical conductivity for the sulfur, and the other is to provide pore structure for the loaded sulfur. Porous carbon delamination improves the conductivity of electrode materials and adsorbs soluble polysulfide ions. However, soluble substances can still flow out of carbon pores, affecting recovery performance. The traditional carbon matrix material system has few kinds and single structure, which can not meet the special design and improvement needs of sulfide composite materials[19].

Metal organic frameworks (MOFs), a new kind of porous framework, is a type of crystalline porous material prepared by coordination of metal ions and organic binder. And MOFs have good pore characteristics, large surface area, relatively stable chemical properties and controllable metal-organic frame structure[16,20]. What's more, the formation of the surface of the composite materials of channel abundant functional groups can load more active substance sulfur adsorption by key materials, helping to suppress elemental sulfur and sulfur compounds are dissolved in the electrolyte, which is beneficial to fully improve lithium sulfur batteries cycle performance and maintain the higher the positive materials of the active material utilization. Man Gao et al. [21] phosphorylated the precursors of Prussian blue@graphene oxide and prepared the FeP composite material with double carbon coating in situ. When the product is used as the positive electrode material of lithium-ion batteries, the specific capacity is maintained at about  $830 \text{ mAh g}^{-1}$  after 100 cycles at the current of  $100 \text{ mA g}^{-1}$ , while at  $5 \text{ A g}^{-1}$  current,  $359 \text{ mAh g}^{-1}$  can be obtained.

Although MOF has these advantages, the electronic conductivity of MOF is poor [19], which limits its electrochemical performance. For example, an electrochemically active MOF (MOF-5) has an electrical conductivity of  $1.0 \times 10^{-4} \text{ S/cm}$  [22] at normal temperature and another MOF ( $\text{Cu}[\text{Ni}(\text{pdt})_2]$ ) at normal temperature. The conductivity is only  $1.0 \times 10^{-8} \text{ S/cm}$  [23]. In order to solve the problem of poor conductivity of MOF, it is fully utilized in the cathode material of lithium-sulfur battery. Some researchers have used MOF material as precursor, and realized the application of MOF in lithium-sulfur battery by high-temperature carbonization. For the first time, Xi et al. [24] prepared mesoporous carbon material sulfur composites by carbonizing four mesoporous metal organic framework materials. During the process of carbonization from mesoporous MOF to mesoporous carbon, the porous structure of the material is well retained, and the rich pore volume and pore size distribution after carbonization effectively increase the sulfur loading and cycle performance of the material. In the process of carbonization, the porous material is transformed from a poorly conducting mesoporous to a mesoporous carbon with good conductivity. Although the conductivity of the

composite material is improved to a certain extent, the overall conductivity of the material is still not excellent. After the cycle 40 times, the capacity was only maintained at 592 mA h g<sup>-1</sup> the capacity retention ratio was low, and the electrochemical property of the composite was not fully exerted. Liu et al. [25] selected a metal-organic framework—ZIF-8, which is mainly composed of micropores, as a carbonization template and skeleton, and injected sulfur into the porous skeleton to obtain an S/MPCP composite. At a ampere density of 100 mA g<sup>-1</sup>, the first discharge specific capacity was 920 mA h g<sup>-1</sup>, and the capacity after this cycle was 490 mA h g<sup>-1</sup>, showing a high capacity retention ratio and good cycle performance. However, compared to the existing specific capacity of the sulfur-carbon composite, the specific capacity level is still low.

In order to ensure the excellent electron conduction and ion migration with the charge and discharge, we added different proportions of CNTs in the MOF (MIL-101(Cr)) to increase its conductivity. MIL-101 (Cr)/CNT/S composite anode material has been successfully prepared, and the weight ratio of CNTs was 2%, 5% and 7%. In addition, the effect of CNTs content on the electrochemical property of sulfur electrode materials and the application of MIL-101(Cr) in lithium-sulfur batteries were studied.

## 2. EXPERIMENTAL

### 2.1. Preparation of the modified Chromium-Metal–Organic Frameworks (MIL-101(Cr)/CNT)

MIL-101 (Cr)/CNT was prepared by a simple hydrothermal reaction method. Typically, take 0.996 g terephthalic acid and 2.4 g Cr (NO<sub>3</sub>)<sub>3</sub>9H<sub>2</sub>O, and some carbon nanotubes, the weight of carbon nanotubes is 2 %,5%,7% of the pure MIL-101 (Cr) , fully ground into 30mL deionized water and stir for 30 minutes. Then, add 0.1 ml of hydrofluoric acid into the mixed solution and transferred it to 60 ml Teflon lined stainless steel bomb and 8 hours of 220°C. In order to thoroughly remove unreacted terephthalic acid cavities of MIL-101 (Cr), filter residue was transferred to a 60 ml Teflon lined stainless steel bomb and 8 hours of 120°C. After cooling, the crystallized green powder was forward purified by alternating washing with deionized water, DMF and ethanol. Finally, MIL-101 (Cr)/CNT is collected through centrifugal 60°C and vacuum drying 12 hours under at 60°C.

### 2.2. Preparation of the MIL-101(Cr)/CNT/S cathode.

The MIL-101(Cr)/CNT/S composites were obtained by the traditional melt diffusion technique. Typically, the prepared MIL-101(Cr)/CNT and sublimed sulfur were ground together for 20 minutes at a mass proportion of 3:7 and put into 50-mL Teflon-lined stainless-steel bomb keeping at the temperature of 155°C for 20 hours. Finally, the MIL-101(Cr)/CNT/S composites were prepared.

To prepare the electrode, the MIL-101(Cr)/CNT/S composite, super P, and polyvinylidene fluoride (PVDF) at the weight ratio of 7:2:1 mixed together and stirred for 20 hours in a phial with N-methyl-2-pyrrolidone (NMP) being the solvent. Then, the mixed slurry was evenly coated on the Al foil and dried at 55°C for 12 hours in vacuum obtaining the cathode film. The prepared cathode film

was punched into 9-mm diameter discs. The load of the active material was approximately 1–2 mg cm<sup>-2</sup> on every cathode plate[1].

### 2.3 Materials characterization

The phase of all samples were analysed by X-ray diffraction (XRD) using a Bruker D8 Advance diffractometer with Cu K $\alpha$  radiation from 5° to 80° (Rigaku Corporation Tokyo, Japan). The surface images of the MIL-101(Cr) and MIL-101(Cr)/S cathode were acquired by using scanning electron microscopy (SEM; JSM-6700F, JEOL, Tokyo, Japan) at 20 kV.

### 2.4 Electrochemical characterization

The electrochemical performances of the MIL-101(Cr)/S, MIL-101@2%CNT/S, MIL-101@5%CNT/S and MIL-101@7%CNT/S composites were tested through the assembly of CR2025 coin cells. The Celgard 2400 and 15.8 mm lithium foil serve as the separator and counter electrodes, respectively. The electrolyte was composed of 1M lithium hexafluorophosphate (LiTFSI) 1, 3-dioxolane (DOL) and DME (1:1 by volume) with 2 wt% LiNO<sub>3</sub> being the additive. 20  $\mu$ L of electrolytes per gram of sulfur were added to each cell. The charge-discharge performances were tested by LAND-CT2001A battery test instruments within the voltage range of 1.7 to 2.8 V (vs. Li/Li<sup>+</sup>) at different current rates (1C = 1672 mA g<sup>-1</sup>).

## 3. RESULTS AND DISCUSSION

### 3.1 Materials characterization

According to Figure 1, MIL-101 has two obvious diffraction peaks around 5° to 10°, which is consistent with the results of Xueyi He, Eman Elsayed, Bingqiong Tan et al[13,26-28], indicating that MIL-101 has been successfully prepared. With the rise of the addition of CNT, the two diffraction peaks were significantly weakened, which indicates that the addition of CNT reduced the crystallinity of MIL-101. In addition, it can be seen from the diffraction pattern of mil-101 @7%CNT/S that there is an additional diffraction peak of C at the position of 26°, indicating that the amount of CNT added at this time is too large, so that CNT cannot be evenly distributed in the gaps and channels of MIL-101 (Cr).

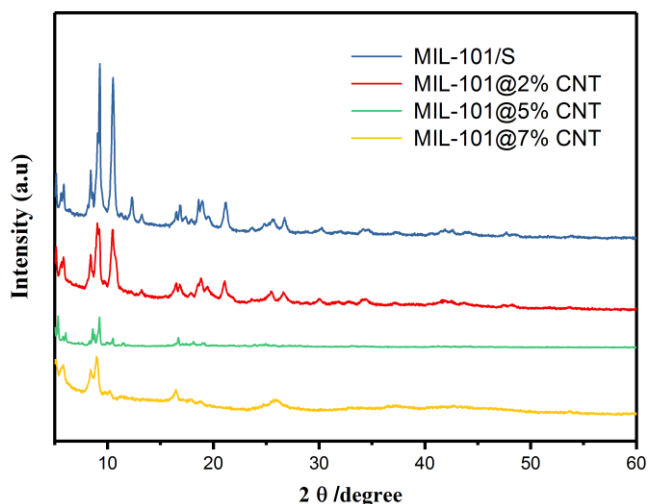


**Figure 1.** X-ray diffraction patterns of MIL-101/S, MIL-101@2%CNT/S, MIL-101@5%CNT/S and MIL-101@7%CNT/S composite

Figure 2 is the SEM image of MIL-101 (Cr) and MIL-101@5%CNT/S. It can be seen from Figure 2(a) that MIL-101 (Cr) is composed of particles with a size of about 200nm, with certain agglomeration phenomenon and enough holes after agglomeration. Figure 2(b) and Figure 2(c) are SEM images of MIL-101@5%CNT/S. As shown in Figure 2(c), CNTs are completely distributed in the surface of MIL-101 (Cr). After the addition of CNTs, the agglomerates of MIL-101 (Cr) have weakened to some extent.

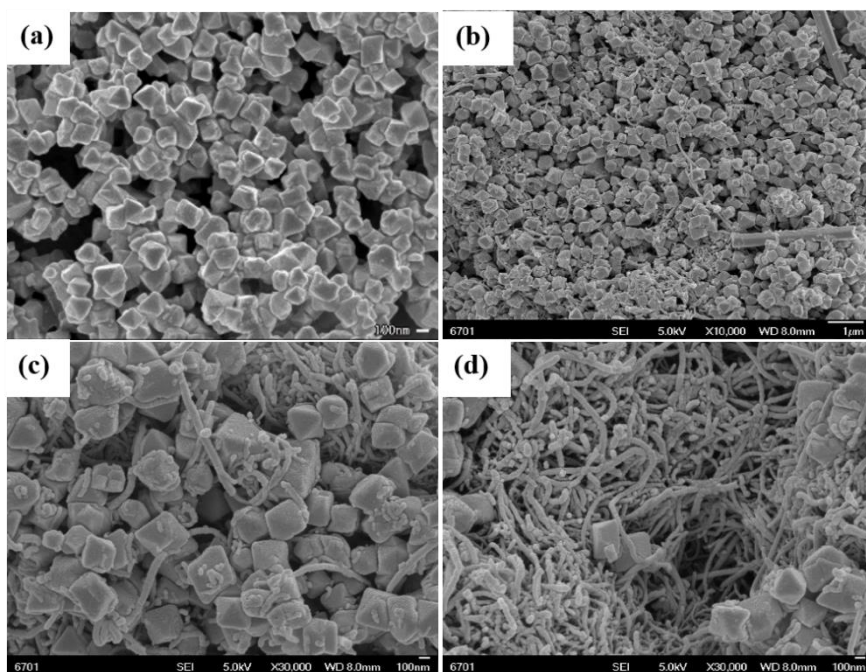


**Figure 2.** (a) SEM images of MIL-101(Cr); (b), (c) SEM images of MIL-101@5%CNT/S; (d) SEM images of MIL-101@7%CNT/S.

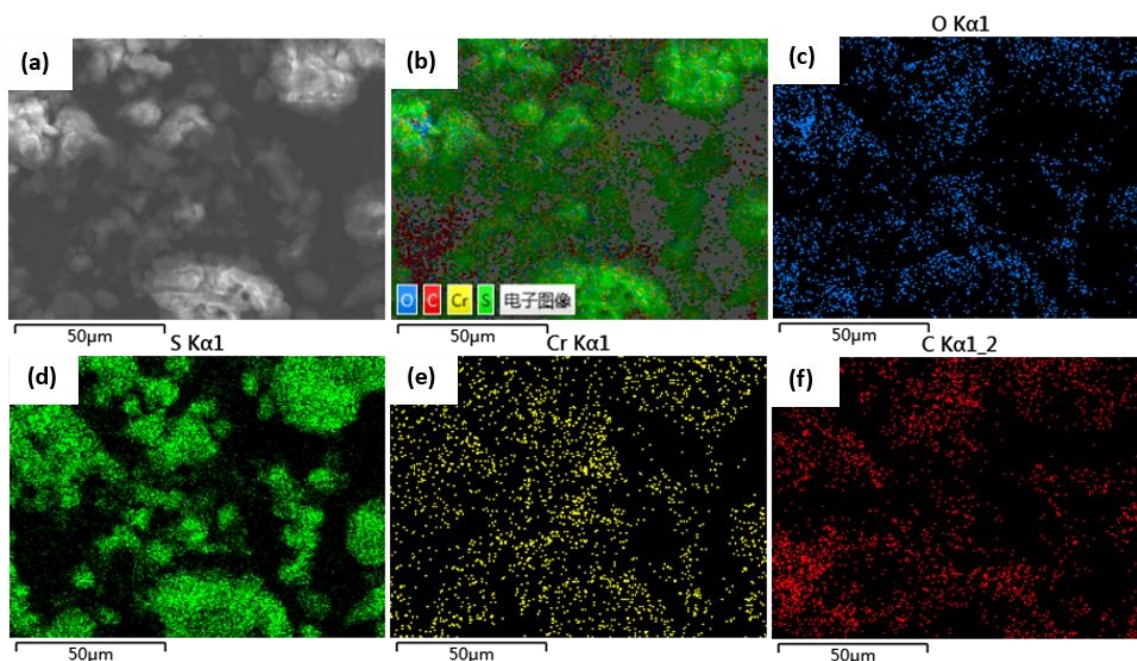


**Figure 3.** (a) , (b) EDS layered image, electronic image of MIL-101@5% CNT/S; (c), (d), (e),(f) EDS mappings showing the distribution of O, S,Cr,C and O;

It is shown in Figure 3(f) that the C element is highly evenly distributed in the MIL-101@5% CNT/S powder, which again demonstrates that the carbon nanotubes are evenly distributed in the voids and pores of the MIL-101. However, as can be seen from Figure 2(d), when too many carbon nanotubes are added, agglomeration of carbon nanotubes occurs.

### 3.2 Electrochemical performance

Figure 4(a) is the Initial discharge-charge currents of MIL-101/S, MIL-101@2% CNT/S, MIL-101@5% CNT/S and MIL-101@7% CNT/S cathodes at a ampere density of 0.1C. Figure 4(b) is the Rate performance of MIL-101 /S, MIL-101@2% CNT/S, MIL-101@5% CNT/S and MIL-101@7% CNT/S cathodes at various current densities. According to Figure 4(a), with the current density being 0.1C, the discharge specific capacity of MIL-101/S, MIL-101@2% CNT/S, MIL-101@5% CNT/S, MIL-101@7% CNT/S positive electrode first turn is 1165.5 mA h g<sup>-1</sup>, 1073.2 mA h g<sup>-1</sup>, 1236.7mA h g<sup>-1</sup>, and 908.6mA h g<sup>-1</sup>, respectively. Therefore, the first discharge of MIL-101@5% CNT/S was significantly better than that of MIL-101@2% CNT/S and MIL-101@7% CNT/S.

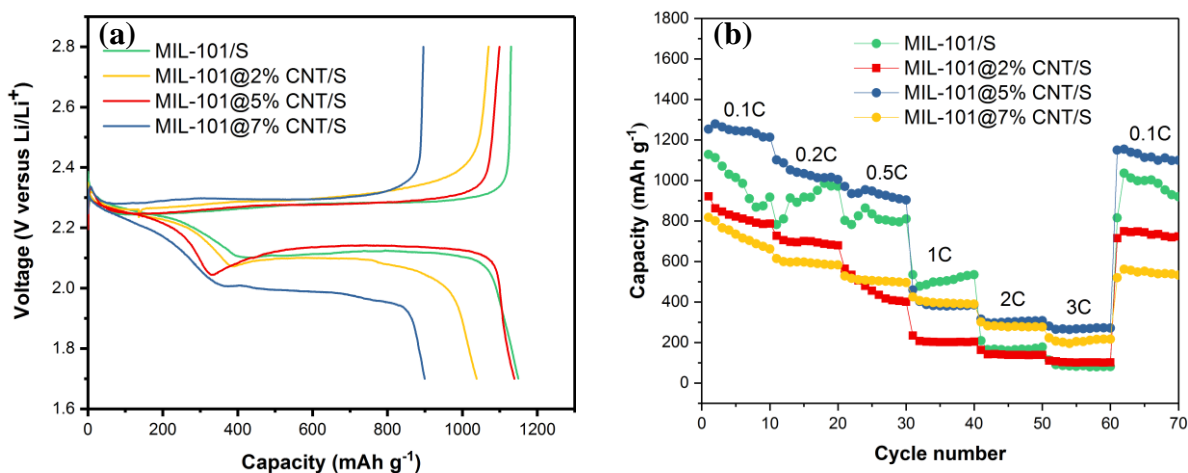


**Figure 4.** (a) Initial discharge-charge currents of MIL-101 /S, MIL-101@2%CNT/S, MIL101@5%CNT/S and MIL-101@7%CNT/S cathodes at a current density of 0.1C; (b) Rate performance of MIL-101 /S, MIL-101@2%CNT/S, MIL-101@5%CNT/S and MIL-101@7%CNT/S cathodes at various current densities

As can be seen from Figure 4(a), the charge-discharge curve consists of two voltage platforms. The first voltage platform corresponds to  $S_8$  to open the chain reaction, and generates high-priced polysulfide  $Li_2S_n$  ( $4 \leq n \leq 8$ ), and the second voltage platform reacts to the reduction reaction of high-priced polysulfide  $Li_2S_n$  to generate a low-priced polysulfide  $Li_2S_n$  ( $2 \leq n \leq 4$ ) [29,30]. During charging, due to the low conductivity of the discharge product  $Li_2S_2$  or  $Li_2S$  and it covers on the anode surface, its initial charging voltage needs to overcome a certain potential barrier, in order for  $Li_2S_2$  or  $Li_2S$  to be oxidized into high-priced polysulfides or monosulfur, which is a barb shape shown in the curve [31]. It is also shown in Figure 4(a) that MIL-101/S, the first platform of MIL-101/S anode contributes a high capacity of nearly  $400 \text{ mA h g}^{-1}$ , which also shows that MIL-101 has a good adsorption effect on polysulfide [16]. However, due to MIL-101's poor electrical conductivity, its second platform contributes less than  $700 \text{ mA h g}^{-1}$ . At the same time, it can be observed that too much or too little addition of CNTs is not conducive to improving the conductivity of MIL-101. When the addition of CNTs is 5%, the conductivity of MIL-101 can be improved. At this time, the contribution capacity of the second platform is about  $950 \text{ mA h g}^{-1}$ ,  $250 \text{ mA h g}^{-1}$  higher than that of the second platform of MIL-101/S. This indicates that the addition of appropriate amount of CNTs improves the conductivity of MIL-101 and enhances the electrochemical kinetics of the transformation from  $Li_2S_4$  to  $Li_2S$ . In addition, with the content of CNTs increasing from 2% to 5% to 7%, the discharge platform first increased and then decreased, and the charging platform decreased firstly and then increased, which indicated that with the increase of CNTs, the polarization of the battery would first decrease and then increase, and the overpotential would decrease and then increase. This may be due to the relatively limited pore volume and specific surface area of the material itself, which cannot realize the high loading of active substances [9].

The results of Figure 4(b) show that the discharge specific capacity of MIL-101 @5%CNT/S is higher than that of MIL-101 @2%CNT/S and MIL-101 @7%CNT/S, no matter how large the multiplier is. At low multiplier, MIL-101/S has good multiplier performance from 0.1C to 0.5C, but at

high multiplier, its capacity declines rapidly. The reason is that at high multiplier, the rate of gaining and losing electrons in the outside world is much higher than the rate of electrons supplied by internal electrochemical reactions, leading to rapid polarization inside the battery and reduced discharge capacity. With the addition of CNTs, multiplier performance was improved. The performance of CNTs at 5% is optimal at both low and high multiples. For MIL-101 @ 5% CNT/S positive, the current density of 0.1C, top 10 circle show nearly 1230 mA h g<sup>-1</sup> discharge specific capacity, and then after 20 cycle, current density of 0.5C gained about 920 mA h g<sup>-1</sup> discharge specific capacity, to 1C, which further increases the current density in 40 circle about 390 mA h g<sup>-1</sup> keep discharge specific capacity, increase, the current density to 3C in 60 cycle to keep about 280 mA g h<sup>-1</sup>, showing good cycle performance keep rate and cycle stability. If the ampere density returns to 0.1C, the discharge specific capacity can be restored to about 1120 mA h g<sup>-1</sup>, reaching over 90% of the initial level, showing a small capacity attenuation.

The reason for this may be the following: the addition of CNTs, on the one hand, enhances the electrical conductivity of the composite, which results in higher capacity retention and good cycle performance, and on the other hand, with the addition of CNTs, the metal component content decreases as the crystal density of MIL-101 decreases[16], resulting in a lower volume capacity density. Moreover, when too much CNTs are added, agglomeration occurs, so that the CNTs are not uniformly distributed, so that the performance of the composite material is more prone to CNTs. Therefore, when the addition of CNTs is too much or too little, the performance will be poor.

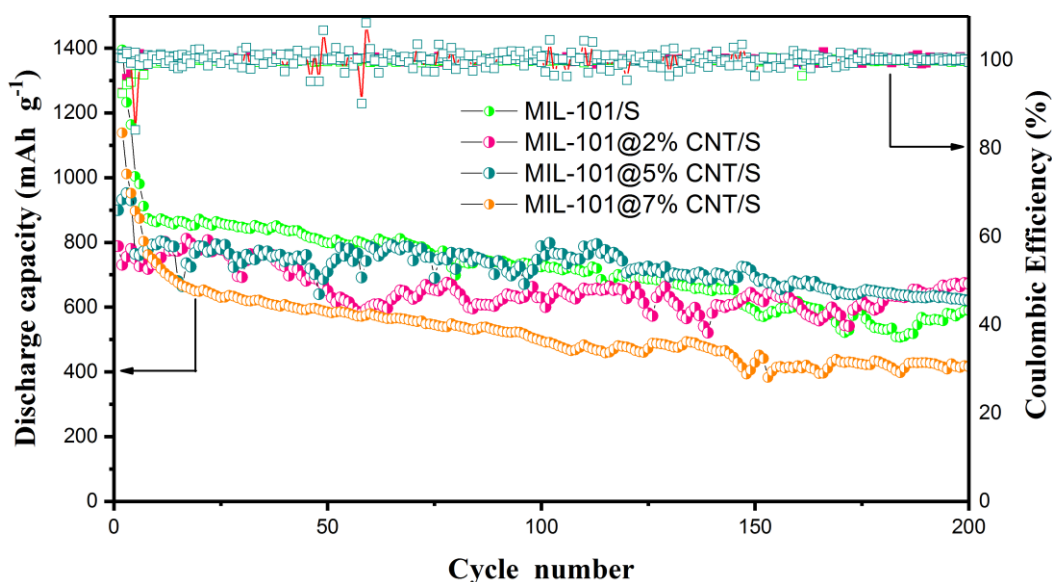


**Figure 5.** Cycling stability of the MIL-101 /S, MIL-101@2%CNT/S, MIL-101@5%CNT/S and MIL-101@7%CNT/S cathodes at a ampere density of 0.1C for 200 cycles

According to Figure 5, the coulombic efficiency is above 95%. When the number of cycles is greater than 75, the discharge specific capacity of MIL-101 @5%CNT/S is higher than MIL-101 /S, and when the number of cycles is more than 175, the discharge specific capacity of MIL-101 @2%CNT/S is higher than MIL-101 /S. When the number of cycles reached 200, the discharge specific capacity of MIL-101 /S, MIL-101@5% CNT/S, andMIL-101@2% CNT/S remained around

630 mAh g<sup>-1</sup>, 660 mA h g<sup>-1</sup>, and 730 mA h g<sup>-1</sup>, respectively. Therefore, the addition of 5% CNTs in MIL-101 (Cr)/S can enhance the utilization rate of active substances and show good cycling performance. The deficiency is that after adding the CNTs to MIL-101 (Cr)/S, the cyclic stability of the anode material decreases, which may be caused by insufficient grinding.

The following table is the performance comparison of MIL-101@5%CNT and other materials in lithium sulfur battery.

**Table 1.** Performance comparison of MIL101@5%CNT and other materials in lithium sulfur batteries

serial number	anode material	initial discharge capacity/current density	cycle-index/curr-ent density	capacity retention ratio
1	MIL-101@5%CNT(this work)	1236.7 mA h g <sup>-1</sup> /0.1C	200/0.1C	53.4%
2	polypyrrole coated hollow MOF[32]	1092.5 mA h g <sup>-1</sup> /0.1C	200/0.1C	32.4%
3	ionic-electronic conducting polymer[15]	1108 mA h g <sup>-1</sup> /0.1C	200/0.1C	64%
4	hierarchical porous nitrogen-doped carbon[33]	1355 mA h g <sup>-1</sup> /0.1C	300/0.2C	38.4%
5	heteroatom-doped porous carbon[34]	1185 mA h g <sup>-1</sup> /0.05C	300/0.2C	41.3%
6	N and O dual-doped porous carbon[35]	1338 mA h g <sup>-1</sup> /0.1C	200/0.1C	77.4%

By comparing the two materials with NO. 1 and NO. 2 in the table, it can be seen that the addition of appropriate amount of CNT does improve the electrical properties of the organic metal skeleton, both in terms of initial discharge capacity and cyclic characteristics, and the cycling performance was improved by 64.8%, which proves our conjecture[32]. However, we can know that MIL-101@5%CNT still has some shortcomings in its cycling performance comparing with porous carbon materials[33–35]. And compared with the ionic-electronic conducting polymer, the initial discharge capacity of MIL-101@5%CNT was improved, but the circulating property was decreased[15].

#### 4. CONCLUSION

In conclusion, MIL-101 (Cr)/CNT/S composite anode material has been successfully prepared, and suitable CNTs were added to MIL-101(Cr) to improve the conductivity of MIL-101(Cr). When the adding amount of CNTs is 5%, the composite material has the best performance. It shows a good multiplier performance, and the capacity contributed by the second platform has been greatly improved.

However, it also has some deficiencies: with the addition of CNTs, the crystallization of MIL-101(Cr) is reduced to some extent, and the cycle stability of charge and discharge is also decreased.

#### ACKNOWLEDGEMENT

This work was financially supported by the National Natural Science Foundation of China (Grant No.11264023). This work was supported by the HongLiu first-class disciplines Development Program of Lanzhou University of Technology financially.

**References**

1. W. Su, W. Feng, S. Wang, L. Chen, M. Li, C. Song, *J Solid State Electrochem*, 23 (2019) 2097–2105.
2. X. Sun, Y. Huang, M. Chen, Y. Wang, X. Gao, L. Wang, *Materials Letters*, 232 (2018) 122–125.
3. J. Wang, L. Si, Q. Wei, X. Hong, L. Lin, X. Li, J. Chen, P. Wen, Y. Cai, *Journal of Energy Chemistry*, 28 (2019) 54–60.
4. Y. Yang, C. Chen, J. Hu, Y. Deng, Y. Zhang, D. Yang, *Chinese Chemical Letters*, 29 (2018) 1777–1780.
5. S.-H. Chung, A. Manthiram, *ChemSusChem*, 7 (2014) 1655–1661.
6. R. Van Noorden, *Nature*, 498 (2013) 416–417.
7. E.S. Shin, K. Kim, S.H. Oh, W.I. Cho, *Chem. Commun.*, 49 (2013) 2004–2006.
8. H.S. Ryu, J.W. Park, J. Park, J.-P. Ahn, K.-W. Kim, J.-H. Ahn, T.-H. Nam, G. Wang, H.-J. Ahn, *J. Mater. Chem. A*, 1 (2013) 1573–1578.
9. J.L. Wang, J. Yang, J.Y. Xie, N.X. Xu, Y. Li, *Electrochemistry Communications*, 4 (2002) 499–502.
10. T.-T. Mai, D.-L. Vu, D.-C. Huynh, N.-L. Wu, A.-T. Le, *Journal of Science: Advanced Materials and Devices*, 4 (2019) 223–229.
11. D. Zhang, G. Li, B. Li, J. Fan, X. Liu, D. Chen, L. Li, *Journal of Alloys and Compounds*, 789 (2019) 288–294.
12. J. Liang, Z.-H. Sun, F. Li, H.-M. Cheng, *Energy Storage Materials*, 2 (2016) 76–106.
13. State Key Laboratory of Advanced Processing and Recycling Nonferrous Metals, Lanzhou University of Technology, Lanzhou 730050, China; W. Su, *International Journal of Electrochemical Science*, 13 (2018) 6005–6014.
14. W. Zhang, X. Chen, G. Zhang, S. Wang, S. Zhu, X. Wu, Y. Wang, Q. Wang, C. Hu, *Solar Energy Materials and Solar Cells*, 200 (2019) 109919.
15. P. Han, S.-H. Chung, A. Manthiram, *Energy Storage Materials*, 17 (2019) 317–324.
16. H. Yang, W. Cui, Y. Han, B. Wang, *Chinese Chemical Letters*, 29 (2018) 842–844.
17. V. Soundharajan, B. Sambandam, J. Song, S. Kim, J. Jo, P.T. Duong, S. Kim, V. Mathew, J. Kim, *Journal of Energy Chemistry*, 27 (2018) 300–305.
18. H. Zhang, Z. Zhao, Y. Liu, J. Liang, Y. Hou, Z. Zhang, X. Wang, J. Qiu, *Journal of Energy Chemistry*, 26 (2017) 1282–1290.
19. R. Demir-Cakan, M. Morcrette, F. Nouar, C. Davoisne, T. Devic, D. Gonbeau, R. Dominko, C. Serre, G. Férey, J.-M. Tarascon, *Journal of the American Chemical Society*, 133 (2011) 16154–16160.
20. K. Zhang, K. Dai, R. Bai, Y. Ma, Y. Deng, D. Li, X. Zhang, R. Hu, Y. Yang, *Chinese Chemical Letters*, 30 (2019) 664–667.
21. M. Gao, X. Liu, H. Yang, Y. Yu, *Science China Chemistry*, 61 (2018) 1151–1158.
22. S. Takaishi, M. Hosoda, T. Kajiwarra, H. Miyasaka, M. Yamashita, Y. Nakanishi, Y. Kitagawa, K. Yamaguchi, A. Kobayashi, H. Kitagawa, *Inorganic Chemistry*, 48 (2009) 9048–9050.
23. Y. Kobayashi, B. Jacobs, M.D. Allendorf, J.R. Long, *Chemistry of Materials*, 22 (2010) 4120–4122.
24. K. Xi, S. Cao, X. Peng, C. Ducati, R. Vasant Kumar, A.K. Cheetham, *Chemical Communications*, 49 (2013) 2192.
25. G. Xu, B. Ding, L. Shen, P. Nie, J. Han, X. Zhang, *Journal of Materials Chemistry A*, 1 (2013) 4490.
26. E. Elsayed, P. Anderson, R. AL-Dadah, S. Mahmoud, A. Elsayed, *Journal of Solid State Chemistry*, 277 (2019) 123–132.
27. X. He, M. Gang, Z. Li, G. He, Y. Yin, L. Cao, B. Zhang, H. Wu, Z. Jiang, *Science Bulletin*, 62 (2017) 266–276.

28. B. Tan, Y. Luo, X. Liang, S. Wang, X. Gao, Z. Zhang, Y. Fang, *Microporous and Mesoporous Materials*, 286 (2019) 141–148.
29. G. Zhou, S. Pei, L. Li, D.-W. Wang, S. Wang, K. Huang, L.-C. Yin, F. Li, H.-M. Cheng, *Adv. Mater.*, 26 (2014) 625–631.
30. Q. (Ray) Zeng, X. Leng, K.-H. Wu, I.R. Gentle, D.-W. Wang, *Carbon*, 93 (2015) 611–619.
31. X. Wang, Z. Zhang, Y. Qu, Y. Lai, J. Li, *Journal of Power Sources*, 256 (2014) 361–368.
32. P. Geng, S. Cao, X. Guo, J. Ding, S. Zhang, M. Zheng, H. Pang, *J. Mater. Chem. A*, 7 (2019) 19465–19470.
33. R. Wu, S. Chen, J. Deng, X. Huang, Y. Song, R. Gan, X. Wan, Z. Wei, *Journal of Energy Chemistry*, 27 (2018) 1661–1667.
34. J. Ren, Y. Zhou, H. Wu, F. Xie, C. Xu, D. Lin, *Journal of Energy Chemistry*, 30 (2019) 121–131.
35. H. Feng, M. Zhang, J. Kang, Q. Su, G. Du, B. Xu, *Materials Research Bulletin*, 113 (2019) 70–76.

© 2020 The Authors. Published by ESG ([www.electrochemsci.org](http://www.electrochemsci.org)). This article is an open access article distributed under the terms and conditions of the Creative Commons Attribution license (<http://creativecommons.org/licenses/by/4.0/>).